Electronic Supporting Information

TiO_2 photoanodes with exposed {0 1 0} facets grown by aerosol-assisted chemical vapor deposition of a titanium oxo/alkoxy cluster

Miriam Regue,[a,b] Sandra Sibby,[b] Ibbi Y. Ahmet,[c] Dennis Friedrich,[c] Fatwa F. Abdi,[c] Andrew L. Johnson*[a,d] and Salvador Eslava*[a,b]

[a]Centre for Sustainable Chemical Technologies, University of Bath, Claverton Down, Bath, BA2 7AY, UK

[b]Department of Chemical Engineering, University of Bath, Claverton Down, Bath, BA2 7AY, UK. E-mail: s.eslava@bath.ac.uk

[c]Helmholtz-Zentrum Berlin für Materialien und Energie GmbH, Institute for Solar Fuels, Hahn-Meitner-Platz 1, Berlin 14109, Germany

[d]Department of Chemistry, University of Bath, Claverton Down, Bath, BA2 7AY, UK

All data created during this research are openly available from the University of Bath data archive at https://doi.org/10.15125/BATH-00644

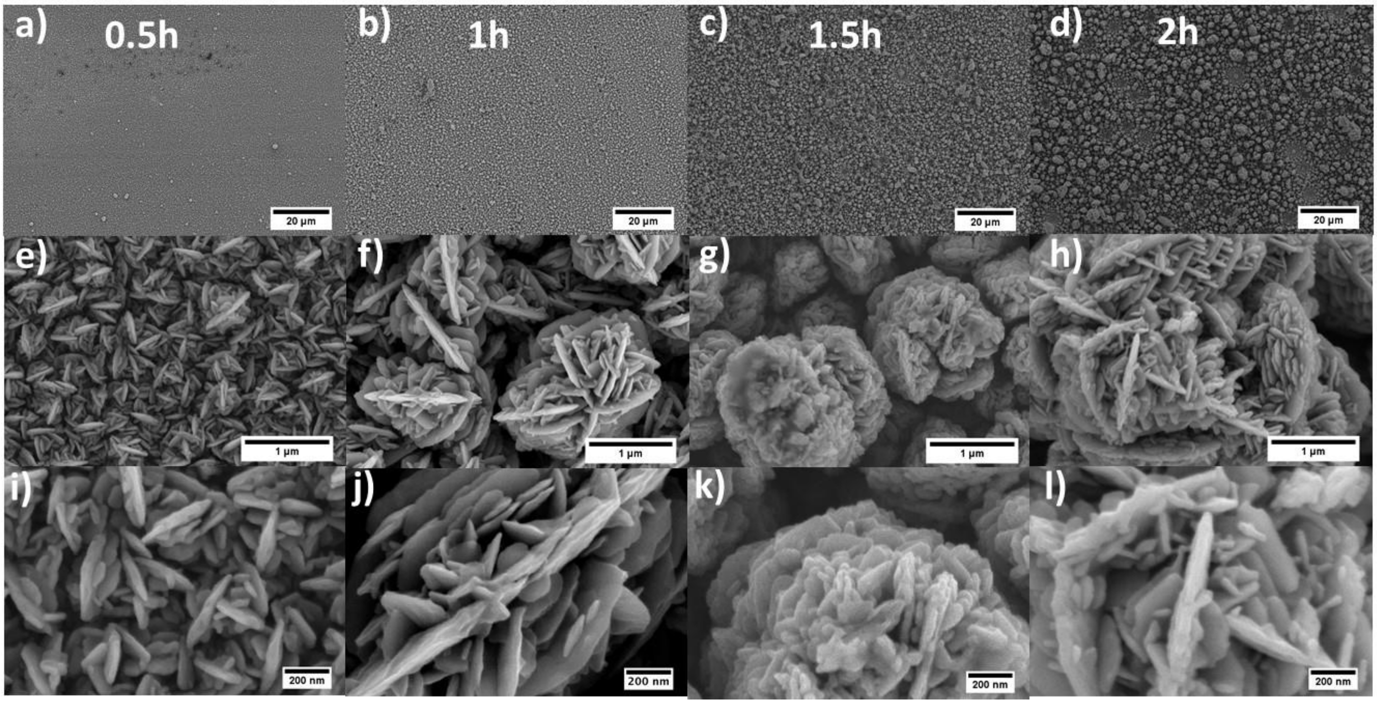

Fig. S1 SEM micrographs at different magnifications of TiO_2-Rose-800 photoanodes deposited at different times (a, e, i) 0.5, (b, f, j) 1, (c, g, k) 1.5 and (d, h, l) 2h on top of FTO-substrates.

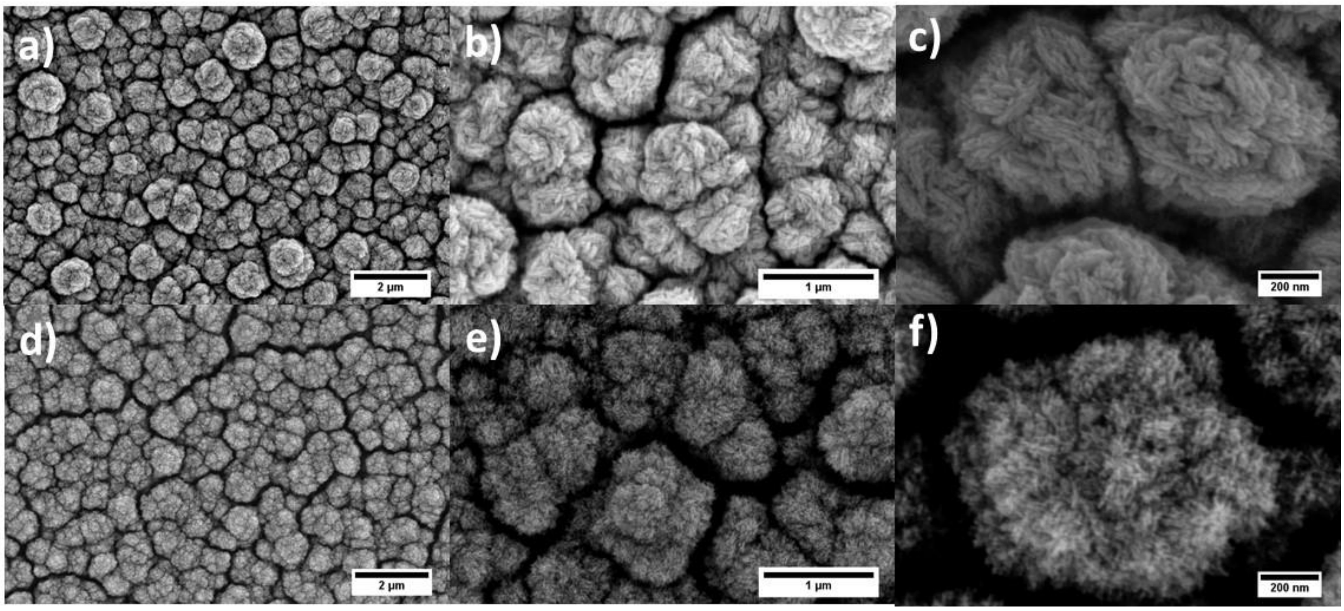

Fig. S2 SEM micrographs at different magnifications of (a-c) TiO_2 deposited at 600°C and (d-f) 700 °C for 1h on top of FTO-substrates.

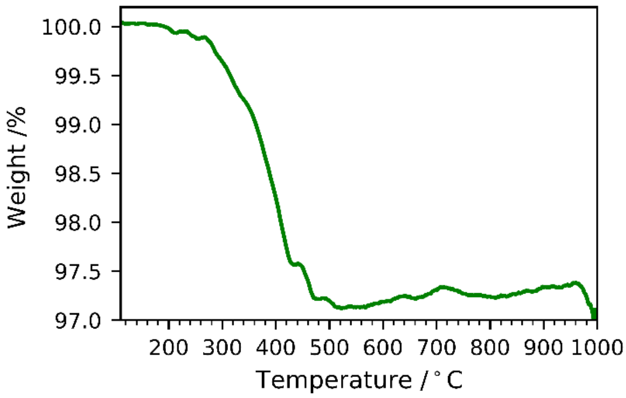

Fig. S3 Thermogravimetric analysis (TGA) in air of TiO_2-Rose-AD on FTO-ABS substrate.

Table S1 Atomic percentage (at%) composition of Ti, O and C of TiO_2 photoanodes.

Sample	Ti (at%)	O (at%)	C (at%)
TiO_2-Rose-800	21.9	59.9	18.2
TiO_2-Rose-AD	12.4	31.2	55.7

Table S2 Ti 2p binding energies

Sample	Ti2$p_{1/2}$ /eV	Ti 2$p_{3/2}$ /eV
TiO_2-Rose-800	463.9	458.2
TiO_2-Rose-AD	465.2	459.4

Table S3 O 1s binding energies of crystal lattice O-Ti^{4+}

Sample	O^{2-}
TiO_2-Rose-800	529.4
TiO_2-Rose-AD	530.7

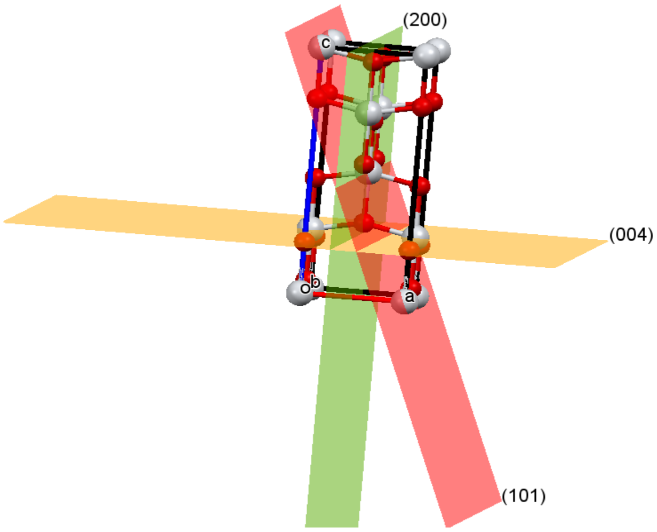

Fig. S4 Anatase TiO_2 crystal structure showing different crystal planes: (0 0 4) in orange, (1 0 1) in red and (2 0 0) in green.

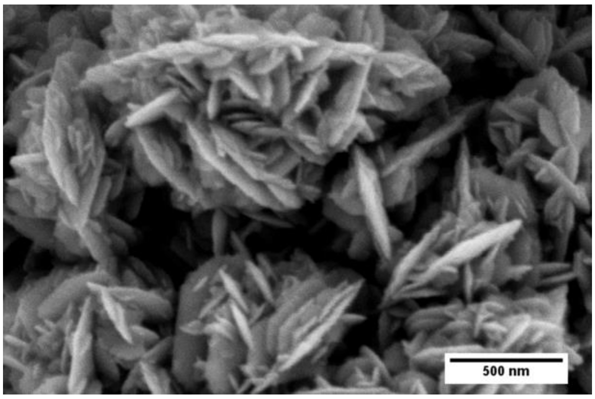

Fig. S5 SEM micrograph of TiO_2-Rose deposited on top of alumina at 500°C.

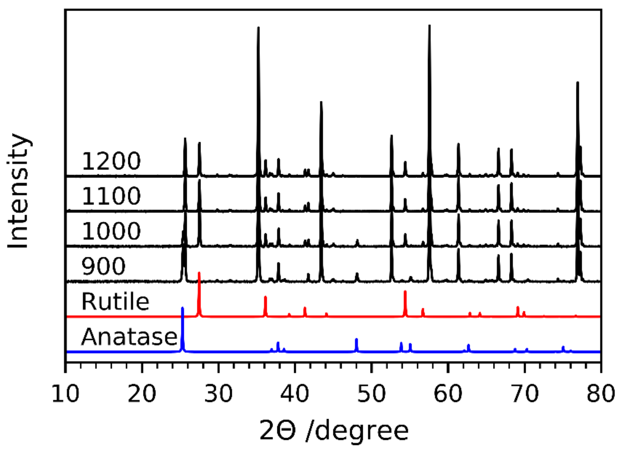

Fig. S6 XRD patterns of TiO_2-Rose on alumina substrates. Standard powder patterns of anatase (blue) and rutile (red) TiO_2 are shown for comparison.

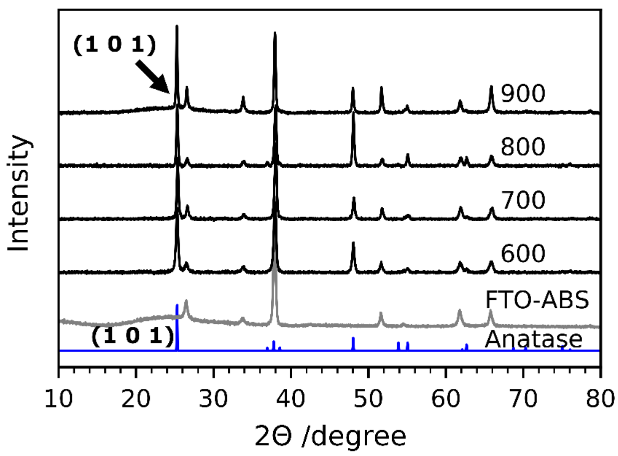

Fig. S7 XRD patterns of TiO_2-Rose films prepared using $Ti_7O_4(OEt)_{20}$ and deposited on FTO-ABS substrate. Standard powder pattern of anatase (blue) TiO_2 and FTO-ABS is also shown.

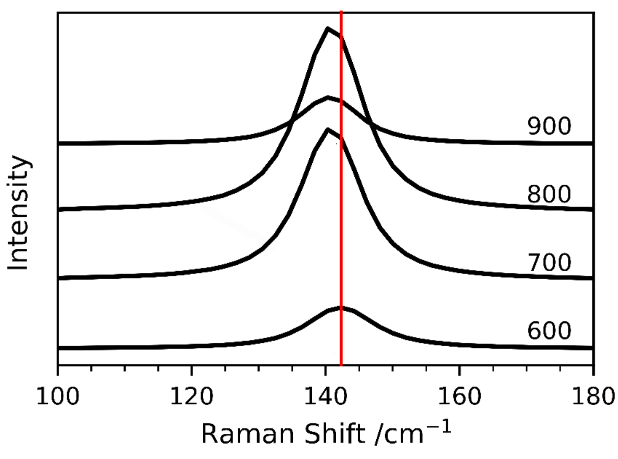

Fig. S8 Raman spectra of E_g Raman mode of anatase TiO_2 (144 cm^{-1}) for TiO_2-Rose prepared using $Ti_7O_4(OEt)_{20}$ precursor and annealed at 600, 700 800 and 900°C for 2h in air.

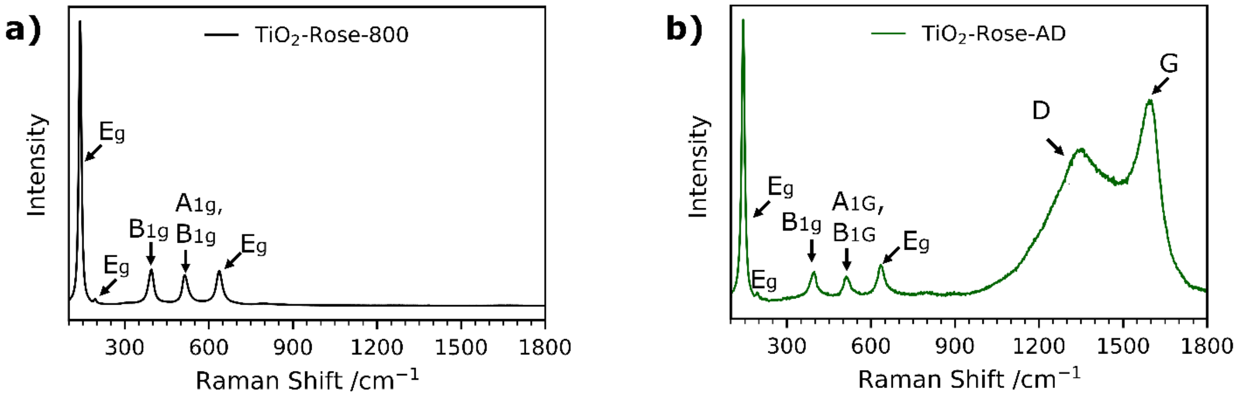

Fig. S9 Raman spectra of (a) TiO_2-Rose-800 and (b) TiO_2-Rose-AD photoanodes.

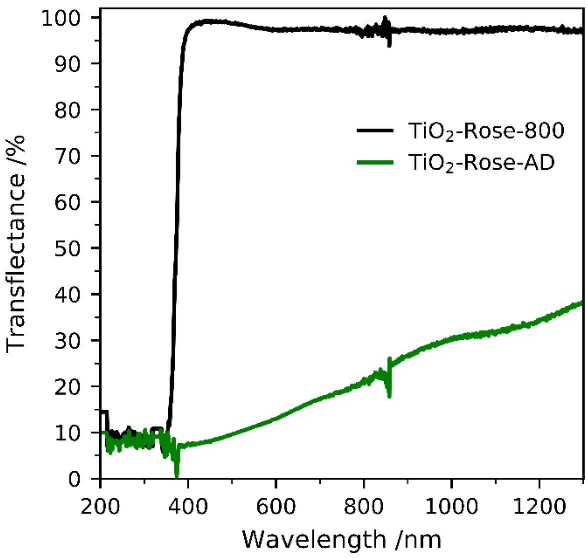

Fig. S10 UV-Vis spectra of TiO_2-Rose-800 and TiO_2-Rose-AD on quartz substrates.

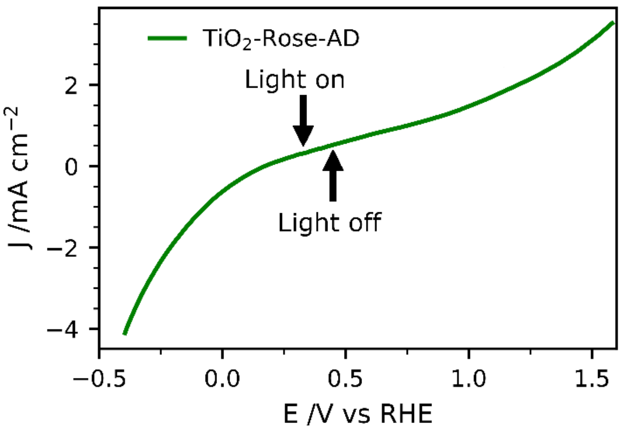

Fig. S11 Photocurrent potential curves of TiO_2-Rose-AD under 1 sun chopped illumination (AM 1.5G, 100 mW cm^{-2}) in 1M KOH (pH=13.7) solution.

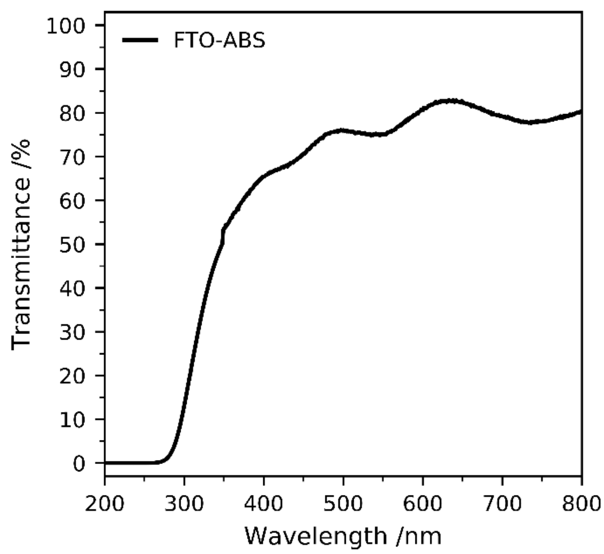

Fig. S12 UV- Vis spectrum of FTO-ABS substrate

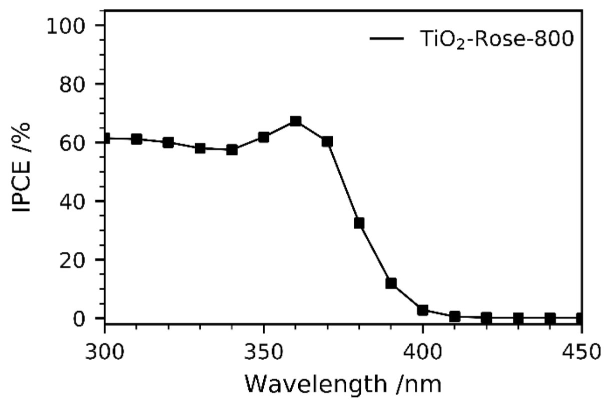

Fig. S13 Front-side IPCE spectra at 1. 23V_{RHE} of TiO_2-Rose-800.

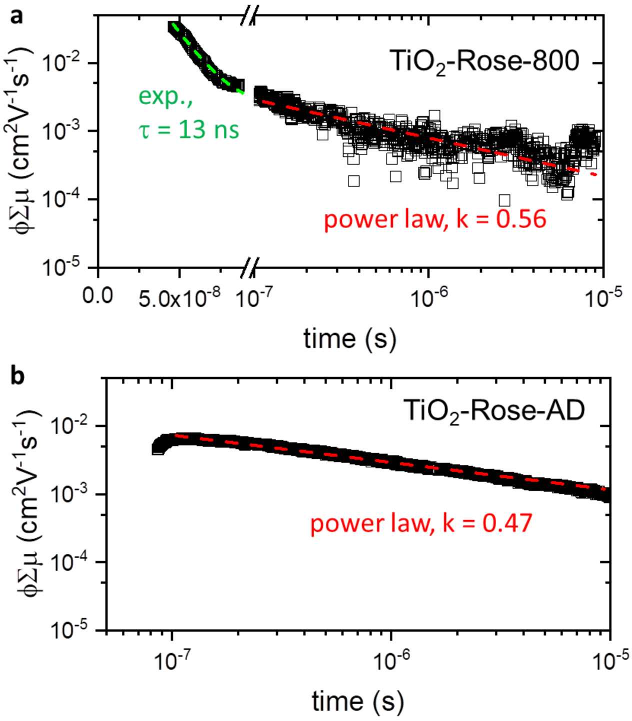

Fig. S14 Fitted curves of time resolved microwave conductance signals for (a) TiO_2-Rose-800 and (b) TiO_2-Rose-AD using a 350 nm laser pulse with a photon flux of 3.97 x 10^{13} photons $cm^{-2}pulse^{-1}$.

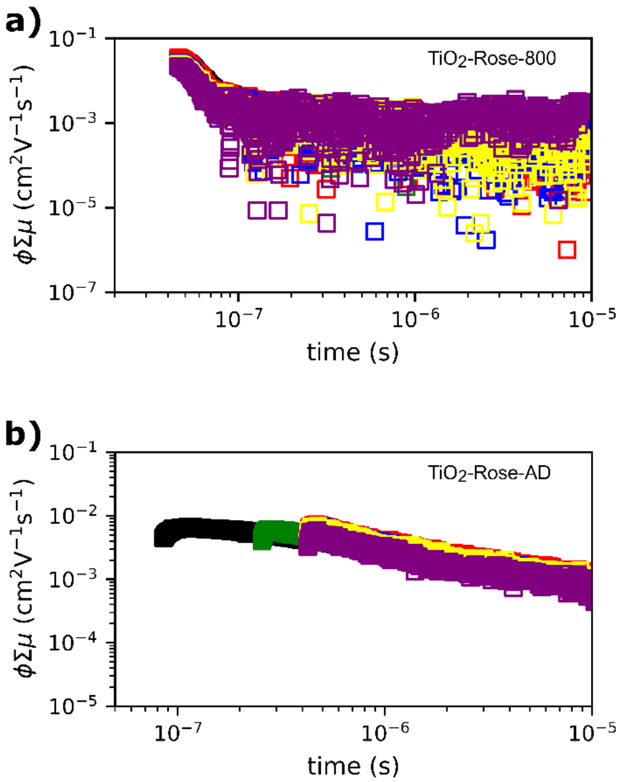

Fig. S15 Time resolved microwave conductance signals for (a) TiO_2-Rose-800 and (b) TiO_2-Rose-AD using a 350 nm laser pulse with various photon flux intensities: 3.97 x 10^{13} (black), 3.11 x 10^{13} (green), 2.0 x 10^{13} (red), 1.80 x 10^{13}(blue), 1.36 x 10^{13}(yellow) and 1.15 x 10^{13} (purple) photons cm^{-2} $pulse^{-1}$.

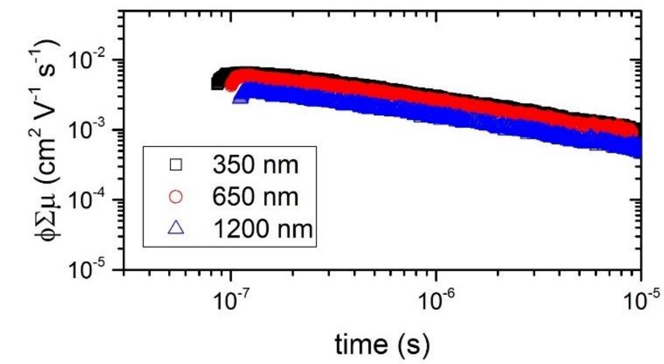

Fig. S16 Time resolved microwave conductance signals for TiO_2-Rose-AD using a 350, 650 and 1200 nm laser pulse with a photon flux of 3.97 x 10^{13}, 2.01 x 10^{14} and 1.22 x 10^{14} photons $cm^{-2}pulse^{-1}$, respectively.

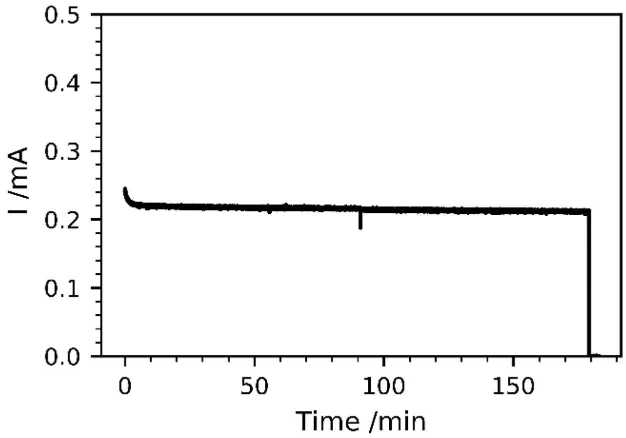

Fig. S17 Photocurrent-time curve of TiO_2-Rose-800 obtained during the O_2 measurement experiment at 1.23 V_{RHE}. Simulated sunlight is switched off after 180 min.

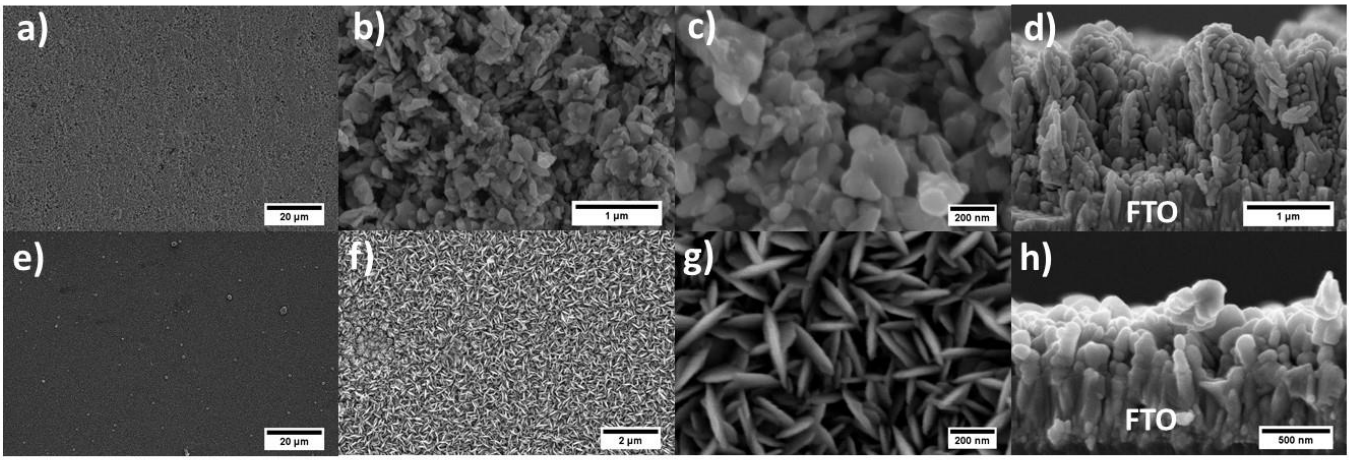

Fig. S18 SEM micrographs at different magnifications of (a-d) TiO_2-0.35M-800 photoanodes and (e-h) TiO_2-0.05M-800 photoanodes on top of FTO-substrates.

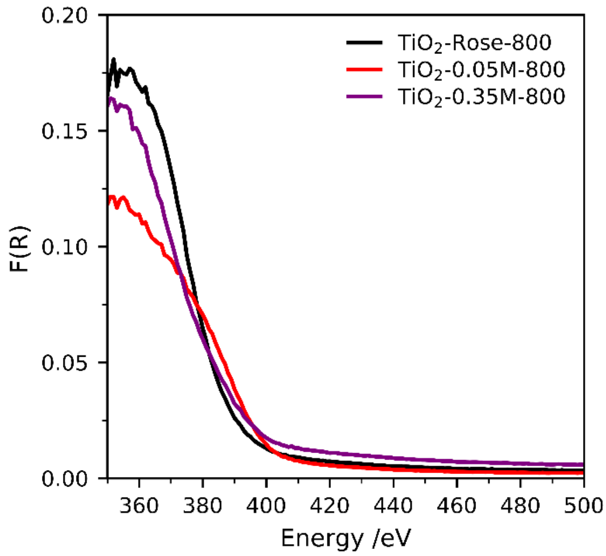

Fig. S19 Diffuse reflectance UV-Vis spectra of TiO_2-Rose-800, TiO_2-0.05M-800 and TiO_2-0.35M-800.

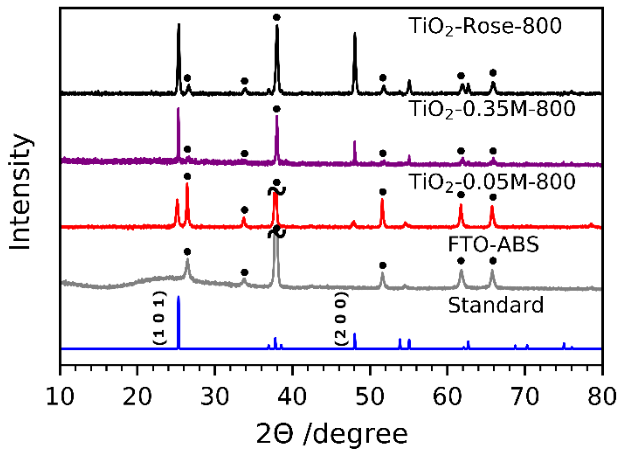

Fig. S20 XRD patterns of TiO_2-Rose-800, TiO_2-0.05M-800 and TiO_2-0.35M-800 TiO_2 films on FTO-ABS substrate. Standard powder patterns of anatase TiO_2 (blue) and FTO-ABS (grey) are also shown for comparison.

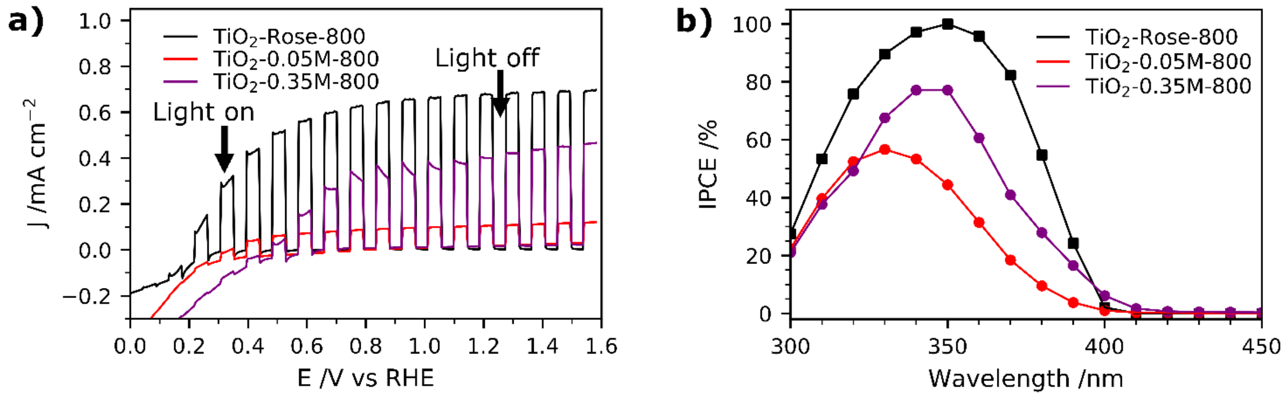

Fig. S21 (a) Photocurrent potential curves of TiO_2-Rose-800, TiO_2-0.05M-800 and TiO_2-0.35M-800 under 1 sun chopped illumination (AM 1.5G, 100 mW cm^{-2}). (b)) IPCE spectra at 1.23 V_{RHE} of TiO_2-Rose-800, TiO_2-0.05M-800 and TiO_2-0.35M-800. All measurements were performed in 1M KOH (pH=13.7).

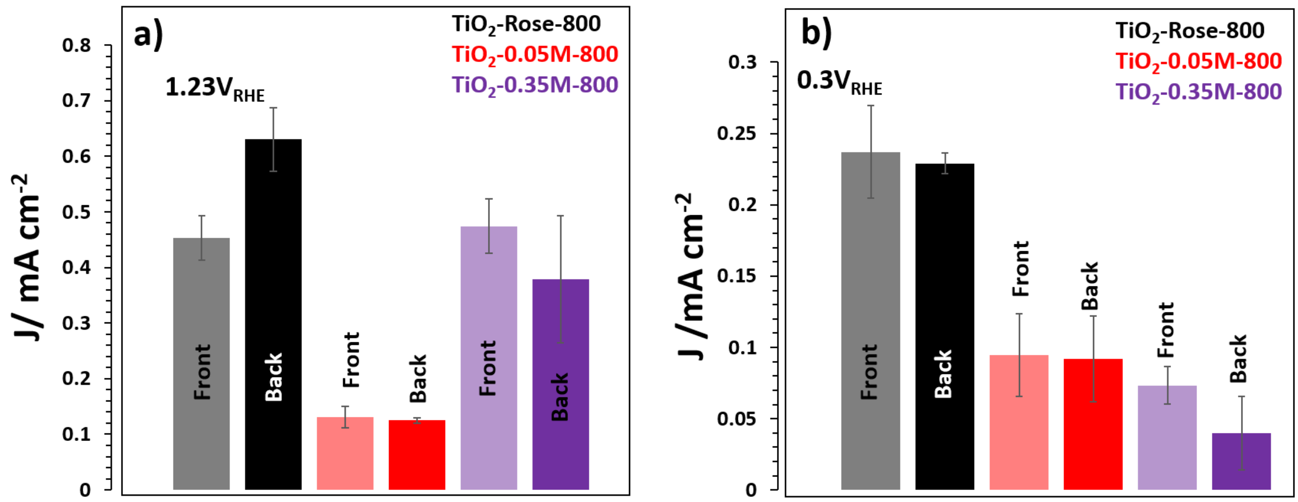

Fig. S22 Photocurrent obtained using front and backside illumination for TiO_2-Rose-800, TiO_2-0.05M-800 and TiO_2-0.35M-800 at (a) 1.23V_{RHE} and (b) 0.3V_{RHE}

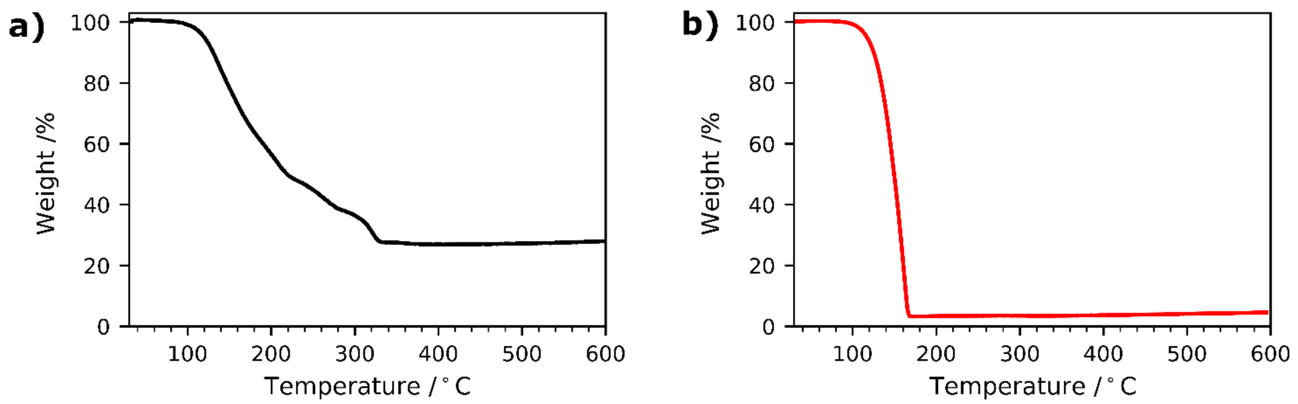

Fig. S23 (a) Thermogravimetric analysis (TGA) in Ar of $Ti_7O_4(OEt)_{20}$ and (b) $Ti(OEt)_4$